2021-07-21

Singlet channel scattering in a Composite Higgs model on the lattice

Drach, V

http://hdl.handle.net/10026.1/17538

Singlet channel scattering in a Composite Higgs model on the lattice

Vincent Drach,[1] Patrick Fritzsch,[1, 2] Antonio Rago,[1] and Fernando Romero-López[3]

[1]*Centre for Mathematical Sciences, Plymouth University, Plymouth, PL4 8AA, United Kingdom*
[2]*School of Mathematics, Trinity College Dublin, Dublin 2, Ireland*
[3]*IFIC (CSIC-UVEG), Edificio Institutos Investigación, Apt. 22085, E-46071 Valencia, Spain*
(Dated: July 22, 2021)

We present the first calculation of the scattering amplitude in the singlet channel beyond QCD. The calculation is performed in $SU(2)$ gauge theory with $N_f = 2$ fundamental Dirac fermions and based on a finite-volume scattering formalism. The theory exhibits a $SU(4) \rightarrow Sp(4)$ chiral symmetry breaking pattern that is used to design minimal composite Higgs models that are tested at the LHC. Our results show that, for the range of underlying fermion mass considered, the lowest flavour singlet state is stable.

PACS numbers:

I. INTRODUCTION

The discovery of the Standard Model (SM) last missing piece, the Higgs boson, and the increase in precision of tests of its properties, continue to trigger the study of numerous mechanisms to address the fundamental problems with its formulation.

Among other possibilities, a new strongly interacting sector giving rise to the observed phenomenology at the electroweak scale and below has been pursued for decades. Such a new sector could feature a solution to the naturalness problem and provide a mechanism to generate non-trivial mass spectrum together with a large scale separation. These mechanisms have been used for instance in the context of Dark Matter models [1, 2], of Composite Higgs models [3–8] or of scenarios of dynamical electroweak symmetry breaking [9, 10]. These appealing ideas motivate the lattice endeavour to understand gauge theories beyond QCD.

One feature of a strongly interacting sector is the inevitable presence of a flavour singlet state of positive parity—referred to as σ in the rest of this paper. In QCD-like theories, the σ is expected to be a resonance of two Goldstone bosons in the limit of massless underlying fermions.

Irrespective of the strong dynamics, the experimental constraints on practical models are derived from the low energy effective theory corresponding to the low energy limit of the strong sector weakly perturbed by its coupling to the SM. The construction of the effective theory at the electroweak scale relies therefore centrally on input from the strongly interacting sector in isolation from the SM. Lattice studies of gauge theories provide robust predictions that can be systematically checked and improved and are therefore crucial to constrain models of physics beyond the SM. In writing such an effective theory, it is for instance often assumed that the contribution of the σ at the electroweak scale is negligible: namely that the scalar state is a heavy resonance that has no effect on the phenomenology. In Composite Higgs scenarios, such a state would mix with the Goldstone Bosons, therefore altering the properties of the physical Higgs bosons and

giving rise to an additional effective scalar field with a larger mass. The resonance is expected to be produced by the LHC in similar fashion to the SM Higgs via gluon fusion and vector boson fusion mechanisms. The phenomenological implications are for instance discussed in Ref. [11]. The present work aims at contributing to understand the role of such a resonance in the phenomenology of models based on strongly interacting sectors.

In lattice simulations the only rigorous approach to reveal the nature of a resonance is to estimate the scattering amplitude of the Goldstone bosons. Lattice simulations in various gauge theories have estimated the mass of the σ in a regime where it is stable, see for instance Refs. [12–22]. Scattering amplitudes have been evaluated also for other channels, see for instance the recent work in a possible nearly conformal theory for $SU(3)$ with $N_f = 8$ flavours in the maximal-isospin channel [23] and our recent work in the vector meson channel for $SU(2)$ with $N_f = 2$ flavours [24].

In this work, we consider an $SU(2)$ gauge theory with $N_f = 2$ fundamental Dirac fermions. The theory features an extended $SU(4)$ flavour symmetry that spontaneously breaks to $Sp(4)$. The theory is used to build a pseudo-Nambu-Goldstone Boson (PNGB) Composite Higgs model in Ref. [25], and it was recently reviewed in Ref. [26]. In this model, the physical Higgs boson is a mixture of PNGBs and of the flavour singlet state of the strong sector. The model has been shown to pass experimental constraints [26], and the mixing between the scalar resonance and the Higgs can relax the bounds on the model [11].

We present here the first calculation of the scattering amplitude of Goldstone Bosons in the flavour singlet channel beyond QCD. We have used two operators to constraint the scattering amplitude at two different kinematic configurations. The evaluation of disconnected contributions increases significantly the computational cost with respect to other channels.

We also report on the comparison of our results to the chiral perturbation theory predictions (in isolation of the SM) of Ref. [27] that should match in the limit of light enough PNGBs.

II. LATTICE SETUP

We use the HiRep [28] suite to simulate an $SU(2)$ gauge theory with $N_f = 2$. For the fundamental fermions the action of choice is the Wilson action [29] with tree-level $O(a)$-improvement clover term [30]. For the gauge we use the tree-level Symanzik improved action [31]. Both the bare mass term, $a\,m_0$, and the Wilson term explicitly break the $SU(4)$ flavour symmetry to a $Sp(4)$ subgroup. All our simulation are performed with periodic boundary conditions in all space-time directions.

Ensemble	L/a	T/a	β	$a\,m_0$	c_{sw}	# configs
Heavy	24	48	1.45	−0.6050	1.0	1980
Light	32	48	1.45	−0.6077	1.0	1160

TABLE I: Simulation parameters in our ensembles.

The ensembles used for this work have been generated for $\beta = 1.45$, and two different values of the bare fermion mass. We denote these ensembles as "light" and "heavy" to reference the different values of the pion mass. Here and in the following, we will make use of the naming convention inherited from QCD, that is, the pseudoscalar PNGB of this theory is referred to as pion. The spatial size of the ensembles has been tuned to obtain a value of $M_\pi L \simeq 5$. All the relevant simulation parameters are given in Table I.

For each ensemble, we compute the PNGB mass, M_π, and the vector mass, M_ρ from Euclidean time dependence of appropriate correlation functions. We also extract the bare pseudoscalar decay constant $F_\pi^{\rm bare}$, which renormalises multiplicatively with the renormalization factor Z_A. For more details about the calculation of these quantities, we refer the reader to Ref. [32]. All our findings are summarised in Table II.

In addition, the non-perturbative determination of Z_A was carried out using the RI'-MOM scheme [33], using the same strategy as in the previous setup [32]. For detailed information about the Z_A determination we refer to Ref. [24], where we estimated $Z_A = 0.8022(3)$ for the value of β of this work.

Ensemble	aM_π	aM_ρ	$aF_\pi^{\rm bare}$	$M_\pi/F_\pi^{\rm bare}$
Heavy	0.2065(12)	0.438(27)	0.0395(9)	5.24(11)
Light	0.1597(18)	0.3864(30)	0.0357(9)	4.36(11)

TABLE II: Pion mass, vector mass and decay constant for our two ensembles.

III. SCATTERING IN $SU(2)$

In this section we will review and extend the necessary theoretical background for this work. In particular we will derive all the group classification needed to evaluate the operators and the associated correlation functions for the singlet channel, as well as the finite-volume scattering formalism and the effective field theory (EFT) description of the relevant scattering amplitude.

A. Flavour singlet operators

We start by considering the flavour symmetries of the $SU(2)$ gauge theory with $N_f = 2$. It can be shown that the massless Lagrangian is symmetric under $SU(4)$ flavour transformation, while the mass term can be shown to be $Sp(4)$ invariant. This means that there exist five broken generators, which correspond to the pseudo-Nambu-Goldstone fields. More specifically, it can be shown that they correspond to the three pions and two dibaryons. In terms of the two fundamental fermion fields u and d, we can construct one-particle operators with the right quantum numbers as follows:

$$
\begin{aligned}
\Pi_{ud}(x) &= u^T(x)(-i\sigma_2)C\gamma_5 d(x), \\
\Pi_{\bar{u}\bar{d}}(x) &= \bar{u}(x)(-i\sigma_2)C\gamma_5 \bar{d}(x)^T, \\
\pi^-(x) &= \bar{u}(x)\gamma_5 d(x), \\
\pi^+(x) &= -\bar{d}(x)\gamma_5 u(x), \\
\pi^0(x) &= \frac{1}{\sqrt{2}}\left[\bar{u}(x)\gamma_5 u(x) - \bar{d}(x)\gamma_5 d(x)\right],
\end{aligned} \tag{1}
$$

where the real and antisymmetric matrix $(-i\sigma_2)$ acts in colour space and C represents the conjugation charge matrix, $C = i\gamma_0\gamma_2$. As we are interested only in the flavour structure of the operators, we will omit the space-time dependence of the fields in the equations where possible.

In order to build a flavour singlet operator, we introduce:

$$
\begin{aligned}
Q &= \begin{pmatrix} u_L \\ d_L \\ \widetilde{u}_L \\ \widetilde{d}_L \end{pmatrix} = \begin{pmatrix} u_L \\ d_L \\ (-i\sigma_2)C\bar{u}_R^T \\ (-i\sigma_2)C\bar{d}_R^T \end{pmatrix}, \\
E &= \begin{pmatrix} 0 & \mathbb{1}_2 \\ -\mathbb{1}_2 & 0 \end{pmatrix},
\end{aligned} \tag{2}
$$

where we used the convention from Ref.[34], summarised in appendix A, together with the standard definition of $q_{L,R} = P_{L,R}\, q$ and $\bar{q}_{L,R} = \bar{q}\, P_{R,L}$ where $P_L = (1 - \gamma_5)/2$ and $P_R = (1 + \gamma_5)/2$.

With the above convention we can define the multiplet $\Pi^{i=1,\dots,5}$ and the singlet $\mathcal{O}_\sigma$ as

$$
\begin{aligned}
\Pi^i &= \frac{1}{2}\left[Q^T(-i\sigma_2)C\gamma_5 X^i EQ + \text{h.c}\right], \\
\mathcal{O}_\sigma &= \frac{1}{\sqrt{2}}\left[Q^T(-i\sigma_2)CEQ + \text{h.c}\right].
\end{aligned} \tag{3}
$$

Here $X^{i=1,\dots,5}$ are the broken generators used to parametrise the coset $SU(4)/Sp(4)$ defined in the appendix.

Considering the infinitesimal transformation

$$Q \longrightarrow \left(\mathbb{1}_4 + i\alpha^a S^a \right) Q, \qquad (4)$$

where $\alpha^{i=1,\dots,10}$ are real parameters, and $S^{a=1,\dots,10}$ are the generators of the Lie Algebra of $Sp(4)$. The generators obey the Lie algebra defining relation:

$$E S^a + (S^a)^T E = 0. \qquad (5)$$

It is straightforward to show that $\mathcal{O}_\sigma$ is a singlet of $Sp(4)$. It can also be shown by performing explicitly an infinitesimal transformation that the multiplet Π transforms as 5-dimensional irreducible representation of $Sp(4)$ and that any operator proportional to $\mathrm{tr}\,[\Pi \otimes \Pi]$ is a singlet of $Sp(4)$. The reader interested in more details is referred to Appendix B.

The operator

$$\mathcal{O}_{\pi\pi} = -\frac{4}{\sqrt{5}} \sum_i \Pi^i \Pi^i \qquad (6)$$

is therefore a flavour singlet operator. Expressing the operator $\mathcal{O}_{\pi\pi}$ in terms of the bilinear defined in Eq. 1, we find:

$$\mathcal{O}_{\pi\pi} = \frac{1}{\sqrt{5}} \Big[+ \pi^+ \pi^- + \pi^- \pi^+ - \pi^0 \pi^0 \\ + \Pi_{ud} \Pi_{\bar{u}\bar{d}} + \Pi_{\bar{u}\bar{d}} \Pi_{ud} \Big]. \qquad (7)$$

Similarly the operator $\mathcal{O}_\sigma$ can be expressed in terms of the u and d fields as:

$$\mathcal{O}_\sigma = \frac{1}{\sqrt{2}} \left[\bar{u}(x)u(x) + \bar{d}(x)d(x) \right]. \qquad (8)$$

In the following, we will use $\mathcal{O}_{\pi\pi}$ and $\mathcal{O}_\sigma$ as the relevant operators to study the singlet channel. We refer to them respectively as the two-pion and sigma operators.

B. Contractions

In the rest of the paper we will use the zero momentum projection of the operators defined in Eq. 1 for the evaluation of the correlators. Explicitly, this is given by

$$\Pi_{ud}(t) = \sum_{\mathbf{x}} \Pi_{ud}(\mathbf{x}, t), \qquad (9)$$

and analogously for the other one-particle operators.

The energy of the flavour singlet state can be computed from the exponential decay in time of the appropriate correlation functions of the two-pion and sigma operators described in the previous section.

The singlet two-pion operator, with each one-particle operator projected at zero momentum is

$$\mathcal{O}_{\pi\pi}(t_1, t_2) = \frac{1}{\sqrt{5}} \Big[\pi^+(t_1)\pi^-(t_2) + \pi^-(t_1)\pi^+(t_2) \\ - \pi^0(t_1)\pi^0(t_2) \\ + \Pi_{ud}(t_1)\Pi_{\bar{u}\bar{d}}(t_2) + \Pi_{\bar{u}\bar{d}}(t_1)\Pi_{ud}(t_2) \Big], \qquad (10)$$

where we have included the Euclidean time explicitly. Analogously, the zero momentum projected sigma operator can be rewritten as

$$\mathcal{O}_\sigma(t) = \frac{1}{\sqrt{2}} \sum_{\mathbf{x}} \left(\bar{u}(\mathbf{x},t)u(\mathbf{x},t) + \bar{d}(\mathbf{x},t)d(\mathbf{x},t) \right). \qquad (11)$$

Using the two operators in Eqs. 10 and 11, we can build a symmetric two-by-two matrix of correlation functions as follows:

$$C_{X \to Y}(\delta t) = \frac{1}{T} \sum_t \langle O_X(t + \delta t) O_Y(t)^\dagger \rangle. \qquad (12)$$

By solving the associated generalised eigenvalue problem (GEVP) [35], we are able to obtain the energy of the two lowest states in the spectrum, by measuring the exponential decay of the two eigenvalues.

The three different correlation functions that enter in Eq. 12 can be built from eight different Wick contractions:

$$\begin{aligned} C_{\sigma \to \sigma}(t) &= -B(t) + 2\Sigma(t), \\ C_{\pi\pi \to \pi\pi}(t) &= 2D(t) + 3X(t) - 10R(t) + 5V(t), \\ C_{\pi\pi \to \sigma}(t) &= \sqrt{10}\,(T(t) - W(t)). \end{aligned} \qquad (13)$$

These are defined in Fig. 1, along with their naming conventions. Three of the contractions include disconnected diagrams: V, W and Σ, and, as will be seen later, they dominate the statistical uncertainty.

C. Extraction of scattering amplitudes

The Lüscher method [36–38] provides a way to obtain two-particle scattering amplitudes from lattice simulations. The so-called quantization condition connects the finite-volume energy levels to the phase shift. It is a well-established technique [39–47], which has been applied to many systems—see Ref. [48] for a review. In the context of QCD the singlet channel has often been studied, see for example Refs. [49–53].

In the case of two identical scalars with only s-wave interactions, the quantization condition reads [36]:

$$k \cot \delta_0(k) = \frac{2}{\sqrt{\pi}L} \mathcal{Z}_{00}(\eta^2), \quad \eta = \frac{Lk}{2\pi}, \qquad (14)$$

where the energy levels are in the A_1^+ irreducible representation of the octahedral group, and k is the relative momentum in the center-of-mass (CM) frame. Furthermore, $\mathcal{Z}_{00}$ is the standard Lüscher zeta function. Note that in this form, the quantization condition is a one-to-one mapping between an energy level and a point in the phase shift curve.

It is convenient, for our discussion later, to highlight how bound states manifest themselves in the phase shift both at finite and infinite volume.
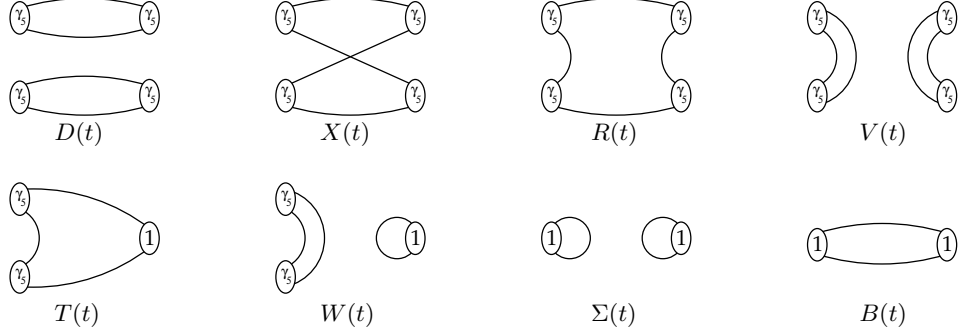
FIG. 1: Representation of the different contractions needed for this work. The blobs indicate a fermion bilinear, with gamma matrix γ_5 or identity. The physical correlation functions are constructed from linear combinations thereof as given in Eq. 13.

In infinite volume, they correspond to poles in the scattering amplitude. The pole's position is given by

$$k \cot \delta_0 (k) = -\sqrt{-k^2}, \tag{15}$$

which we denote as bound-state condition. The fact that residue of the pole has a positive sign, implies the following condition [54]:

$$\frac{d}{dk^2} \left[k \cot \delta_0 (k) - \left(-\sqrt{-k^2} \right) \right] < 0. \tag{16}$$

This means that $k \cot \delta_0$ must cross the bound-state condition from below with decreasing k^2.

By contrast, the finite-volume solutions to the quantization condition never intersect the bound-state condition. They are however exponentially close [55], with an exponent related to the binding momentum [56].

D. EFT prediction

At sufficiently low energies and close to the chiral limit, Chiral Perturbation Theory (ChPT) should provide a satisfactory description of the interactions of Goldstone bosons in QCD-like theories. However, the precise predictions depend upon the symmetry breaking pattern. As explained before, in our case a $SU(4)$ flavour symmetry is spontaneously broken down to $Sp(4)$. This was worked out in Refs. [27, 57], and is referred to as the pseudo-real case.

In the present work the quantity of interest is the two-pion scattering amplitude in the singlet channel—analogous to that of the "σ" resonance in QCD. In this exploratory study, the leading-order (LO) ChPT result will suffice. This reads

$$\mathcal{T}_I = \frac{M_\pi^2}{F_\pi^2} \left(-\frac{3}{2} + 2\frac{s}{M_\pi^2} \right), \tag{17}$$

where we are using the convention $f_\pi = \sqrt{2}F_\pi$ for the normalization of the decay constant, and $\sqrt{s}$ is the CM energy. From the scattering amplitude, the momentum dependence of the phase-shift can be easily derived:

$$\mathrm{Re}\, \frac{1}{\mathcal{T}_I} = \frac{k \cot \delta_0^I}{16\pi\sqrt{s}}. \tag{18}$$

The LO result is

$$\frac{k}{M_\pi} \cot \delta_0^I = \frac{M_\pi \sqrt{s}}{13M_\pi^2 + 16k^2} \left(\frac{32\pi F_\pi^2}{M_\pi^2} \right). \tag{19}$$

Furthermore, the scattering length is defined as

$$\lim_{k \to 0} \frac{k}{M_\pi} \cot \delta_0^I = -\frac{1}{M_\pi a_0^I}, \tag{20}$$

and its result reads

$$M_\pi a_0^I = -\frac{13}{64\pi} \frac{M_\pi^2}{F_\pi^2}. \tag{21}$$

An interesting remark is that the leading-order amplitude has a zero below threshold (Adler zero), which translates into a pole in $k \cot \delta_0^I$. This is located at $(k/M_\pi)^2 = -13/16$, and may limit the converge of a polynomial expansions of $k \cot \delta_0^I$ in k^2—the so-called threshold expansion. Such behaviour has been observed, e.g., in the isospin-2 $\pi\pi$ system in QCD [58].

IV. RESULTS

A. Correlation functions

We construct the correlation functions as indicated in Eq. 13. In order to evaluate all the contractions depicted in Fig. 1, we use various types of stochastic sources. First, for the D, X, R, V and B contractions we use time-diluted stochastic sources. By placing a source in each of the timeslices, we can obtain a single stochastic estimator for each of these contractions. In this case we use 10 stochastic estimators, which require $T \times 10$ inversions of sources. By contrast, we use 40 volume sources for the Σ

contraction, while for W we combine the building blocks of V and Σ. Finally, T is computed by employing 40 time-diluted sources that have an additional sequential inversion.

The contractions Σ and W are responsible for the largest contribution to the statistical uncertainty. This is because they contain the trace of a single propagator multiplied by the identity in spinor space, and so, they are dominated by the gauge noise. Because of this, we choose to measure them more often than the other building blocks. In fact, we measure the trace of the single propagator in steps of one unit of Monte Carlo time.

We perform the analysis of uncertainties using jack-knife samples. In order to account for autocorrelations, we use the binning procedure. For this, we average correlation functions within a bin length of 10 units of Monte Carlo time. We have checked that larger bin sizes, 20 and 30, do not lead to any substantial change in the estimation of uncertainties.

As the operators have vacuum quantum numbers, there is an overall constant in all our correlation functions. Because of this, we will work with the shifted correlator:

$$\widetilde{C}(t) = \frac{1}{2}\big[C(t-1) - C(t+1)\big]. \tag{22}$$

This is a discrete version of the derivative in Euclidean time that keeps the same exponential decay, but cancels the undesired constant.

The results for the two ensembles are shown in Fig. 2. As can be seen, the statistical noise is dominated by the ones including the $\mathcal{O}_\sigma$ operator, which contain the W and Σ contractions in Fig. 1. It is also clear that one cannot trust the correlator in the region dominated by the statistical noise.

B. Spectrum determination

We now turn to the determination of the spectrum. For this, we build a two-by-two matrix, as presented in Eq. 12. The GEVP is defined by means of the shifted correlator as

$$\widetilde{C}(t)v_n(t,t_0) = \lambda_n(t,t_0)\widetilde{C}(t_0)v_n(t,t_0), \tag{23}$$

where t_0 is a reference timeslice. Note that λ_n are the eigenvalues of $\widetilde{C}^{-1}(t_0)\widetilde{C}(t)$. In our case, we choose $t_0 = 4$ as, for both ensembles, it is the first stable point.

There are various ways of solving the eigenvalue equation. One can fix the diagonalisation point, or diagonalise separately in each timeslice. We opt for the latter, but we have seen that it does not lead to any substantial change compared the the other method. Regarding the estimation of uncertainties, we choose to diagonalise in each jackknife sample separately. We have also checked that fixing the diagonalisation in all samples barely alters the outcome.
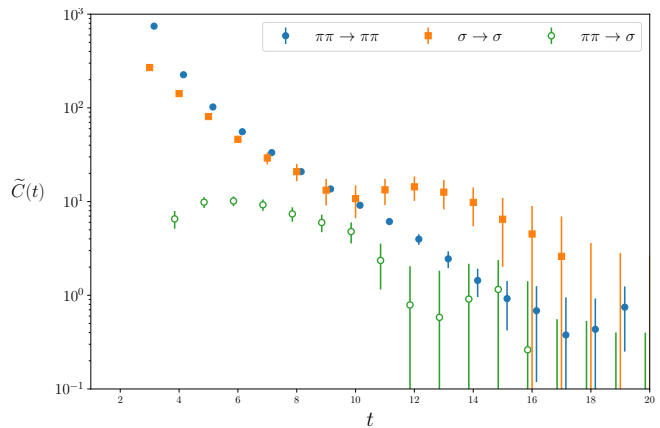
(a)Ensemble with heavier pion mass.
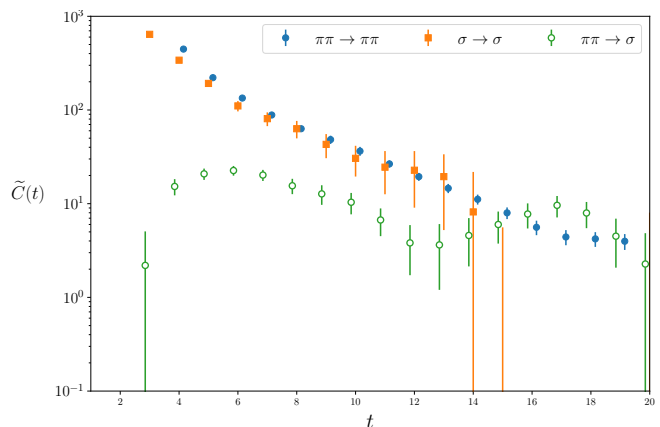
(b)Ensemble with lighter pion mass.

FIG. 2: Correlation functions built with two different operators with singlet quantum numbers. For visualization purposes we include an arbitrary normalization.

The dependence of the eigenvalues with Euclidean time is expected to be a sum of exponentials. Solving the GEVP allows to isolate the low-lying energy states. In the limit of sufficiently large Euclidean time, each eigenvalue decays as a single exponential:

$$\lambda_i(t) \longrightarrow A_i e^{-E_i t}, \tag{24}$$

which holds up to effects that are exponentially suppressed with the time extent of the lattice—thermal effects. The corresponding exponents, E_i, are associated to one energy level of the studied channel.

The dependence of the eigenvalues with Euclidean time is shown in Fig. 3. The dashed lines depict the best fit in the chosen fit interval. Note that we do not include in the fits the region in which the $\widetilde{C}_{\sigma\sigma}$ correlator is dominated by noise.

A summary of the extracted energy levels—in units of the pion mass—is given in Tab. III and in Fig. 4. As can be seen, the central value of the lowest energy is well below threshold, and the second level is around the two-particle threshold in both cases. The physical interpre-
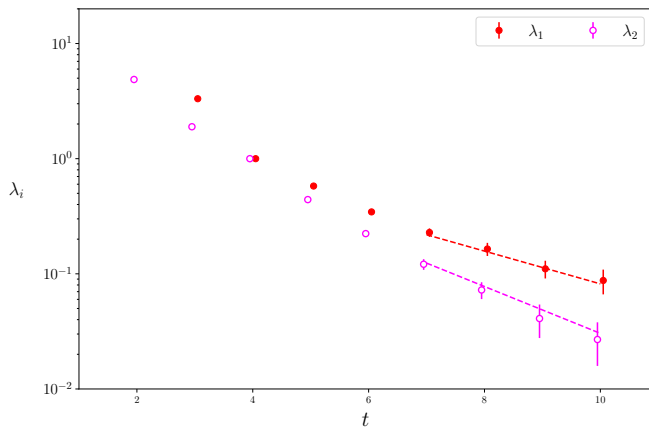
(a)Ensemble with heavier pion mass.
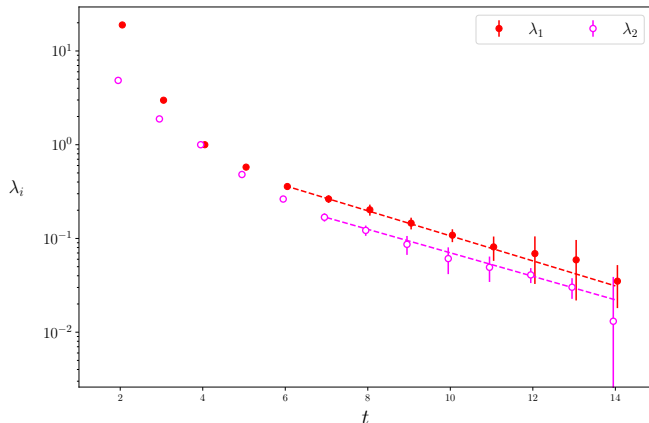
(b)Ensemble with lighter pion mass.

FIG. 3: Lowest two eigenvalues for the two ensembles of this work. The dashed line indicates the fit range.

tation of this states can only be discussed after inspecting the scattering amplitude. In particular, to answer whether the lowest state corresponds to a bound state, or an attractive scattering state. This will be addressed in the next subsection.

Ensemble	E_1/M_π	E_2/M_π
Heavy	1.59(34)	2.27(28)
Light	1.81(22)	1.93(18)

TABLE III: Two-particle energy levels in the singlet channel extracted from the fits in Fig. 3.

C.   Results for the scattering amplitude

We are now in position of exploring the scattering amplitude in the singlet channel using the Lüscher method. For this, we insert the energy levels of Tab. III into the two-particle quantization condition in Eq. 14.

The corresponding points in the phase shift are shown in Fig. 5 for both ensembles, where we also include the 1σ
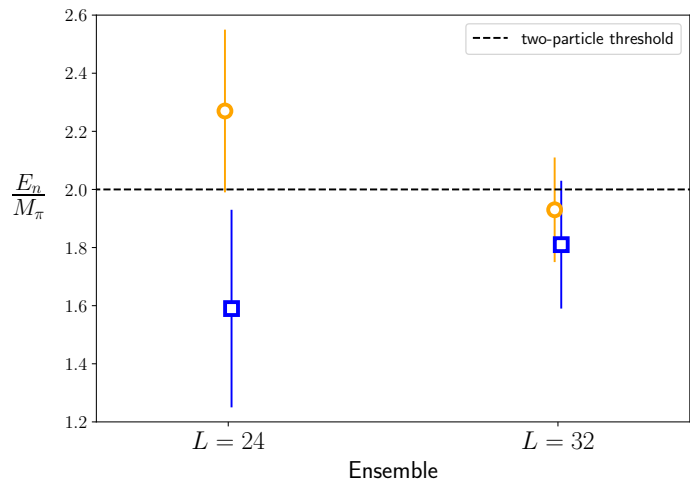
FIG. 4: Energy levels obtained from our simulations.

region for visualization. As can be seen in this figure, we find in both cases a point below threshold whose central value is close to the bound state condition. Even if the uncertainty is large, the most likely interpretation is that there is indeed a bound state in this channel for the explored pseudoscalar mass. The second point in the curve is around threshold, and thus could be used to constrain the scattering length of the channel. Unfortunately the uncertainty is too large, and the result is inconclusive.

We can also comment on the comparison of our results and the leading-order prediction from ChPT. This is depicted as solid grey line in Fig. 5. The LO ChPT prediction shows no sign of a bound state in the region where we seem to find one. It does however predict one bound state well below threshold, which is an artefact caused by the Adler zero [59]. Moreover, the leading chiral prediction is also not able to accommodate the observed points around threshold. Thus, it seems that the value of the pseudoscalar masses of our simulations are outside of the window for which leading-order ChPT is a good description.

V.   CONCLUSION AND OUTLOOK

This work represents the first study of the singlet channel in four-dimensional gauge theories beyond QCD. Specifically, we have considered an $SU(2)$ gauge theory with two fundamental fermions that serves as a minimal template for a Composite Higgs model.

In this theory, the symmetry breaking pattern differs from that of QCD—the $SU(4)$ flavour symmetry breaks down to $Sp(4)$. Therefore, we have derived the group-theoretical setup required to analyse this scattering channel. It can also be noted that our analysis holds for generic $Sp(2N)$ gauge theories with two fundamental fermions as the same symmetry breaking pattern is realised.
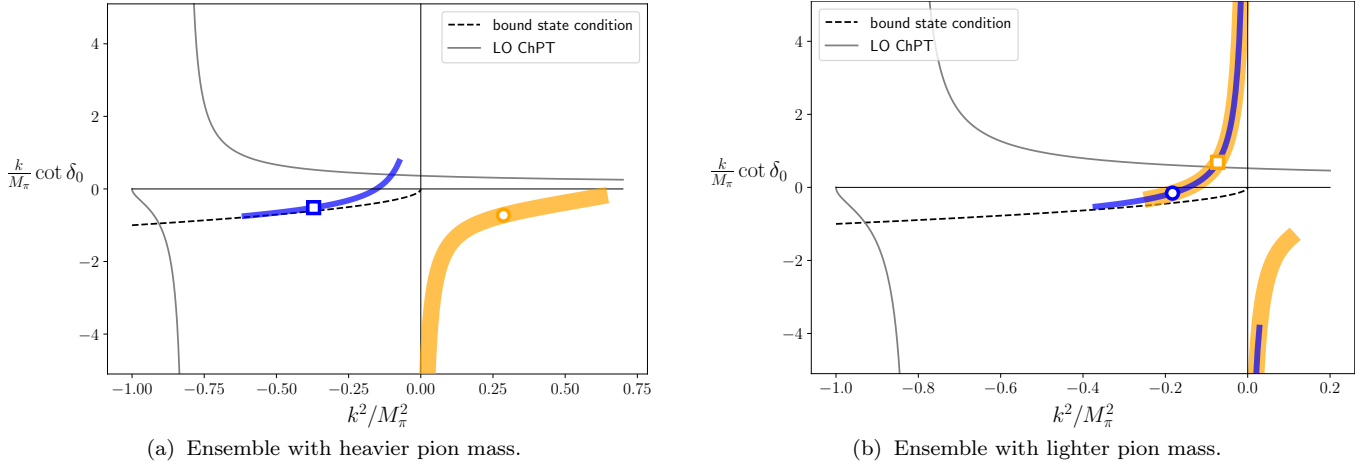
(a) Ensemble with heavier pion mass.

(b) Ensemble with lighter pion mass.

FIG. 5: s-wave phase shift in the form $(k/M_\pi)\cot\delta_0$ for the two ensembles of this work. The empty marker is the central value, as the shaded area represents the 1σ resulting from the quantization condition. Note that the width of the shaded area is arbitrary, and has been chosen for illustrative purposes. We also include the leading-order chiral prediction, as well as the bound-state condition.

We have used two ensembles with different pion masses. Using two different operators to solve the GEVP, we have computed the lowest two energy levels. These are fed into the Lüscher quantization condition, and we have been able to put non-perturbative constraints to the singlet scattering amplitude. Interestingly, we find that leading-order chiral perturbation theory does not seem to describe the amplitude correctly, and fails in predicting a bound state around the region where we observe it.

Our results strongly suggest that in the explored region of fermion masses the sigma is most likely a stable particle, that is, a two-pion bound state. We however expect this feature to depend strongly upon the pion mass. Therefore, more work is required to investigate discretisation effects and to reach the phenomenologically appealing region, that is, where the sigma becomes unstable. We expect to pursue this direction in a subsequent work.

Appendix A: Lie algebra of $SU(4)$

Following the convention used in Ref. [34], we define

$$B_1 = \sigma_4, B_2 = i\sigma_4, B_3 = \sigma_3, B_4 = i\sigma_3,$$
$$B_5 = \sigma_1, B_6 = i\sigma_1, D_4 = \sigma_2, D_5 = i\sigma_2, \tag{A1}$$

where σ_4 is the identity matrix, and $\sigma_{i=1,\dots,3}$ are the Pauli matrices. The ten generators of $Sp(4)$ are denoted $S^{a=1,\dots,10}$, together with the five broken generators $X^{i=1,\dots,5}$ they are a basis of the Lie Algebra of $SU(4)$. They are defined as follows:

$$S^a = \frac{1}{2\sqrt{2}} \begin{pmatrix} \sigma_a & 0 \\ 0 & -\sigma_a^T \end{pmatrix}, \quad a = 1, \dots, 4$$

$$S^a = \frac{1}{2\sqrt{2}} \begin{pmatrix} 0 & B_{a-4} \\ B_{a-4}^\dagger & 0 \end{pmatrix}, \quad a = 5, \dots, 10$$

$$X^i = \frac{1}{2\sqrt{2}} \begin{pmatrix} \sigma_i & 0 \\ 0 & \sigma_i^T \end{pmatrix}, \quad i = 1, \dots, 3$$

$$X^i = \frac{1}{2\sqrt{2}} \begin{pmatrix} 0 & D_i \\ D_i^\dagger & 0 \end{pmatrix}, \quad i = 4, 5. \tag{A2}$$

The generators S^a satisfy the relation $(S^a)^T E + E S^a = 0$. The generators are normalised so that:

$$\text{tr}\left[S^a S^b\right] = \frac{1}{2}\delta^{ab}, \quad \text{tr}\left[X^i X^j\right] = \frac{1}{2}\delta^{ij},$$
$$\text{tr}\left[S^a X^i\right] = 0. \tag{A3}$$

The structure constants of the algebra of $Sp(4)$ are defined as $f_{abc} = 2\text{tr}\left[S^a[S^b, S^c]\right]$.

Appendix B: Transformation under the flavour symmetry group $Sp(4)$

Using the following relations:

$$\{C, \gamma_5\} = 0, \quad C^T = -C,$$
$$C^2 = 1, \quad (-i\sigma_2)^2 = -1, \tag{B1}$$

and the definitions of the Goldstone bosons interpolating fields in Eqs. 1 we find that:

$$\Pi = \frac{1}{2}\left[Q^T(-i\sigma_2)C\gamma_5 X^i E Q + \text{h.c}\right]^{i=1,\dots,5}$$

$$= \frac{1}{2\sqrt{2}} \begin{pmatrix} \pi^- - \pi^+ \\ i(\pi^- + \pi^+) \\ \sqrt{2}\pi^0 \\ i\left(\Pi_{\bar{u}\bar{d}} + \Pi_{ud}\right) \\ \Pi_{\bar{u}\bar{d}} - \Pi_{ud} \end{pmatrix}. \tag{B2}$$

Performing an infinitesimal transformation $Q \longrightarrow Q + i\alpha^a S^a$ where α^a are real infinitesimal parameters, we find that

$$\Pi \longrightarrow \Pi + M\Pi, \quad \text{with}$$

$$M = \sqrt{2} \begin{pmatrix} 0 & -\alpha^3 & -\alpha^2 & -\alpha^7 & \alpha^8 \\ \alpha^3 & 0 & -\alpha^1 & -\alpha^6 & -\alpha^5 \\ \alpha^2 & \alpha^1 & 0 & \alpha^9 & -\alpha^{10} \\ \alpha^7 & \alpha^6 & -\alpha^9 & 0 & \alpha^4 \\ -\alpha^8 & \alpha^5 & \alpha^{10} & -\alpha^4 & 0 \end{pmatrix}. \tag{B3}$$

Here, M is an antisymmetric matrix that can be decomposed onto the algebra of $SO(5)$, therefore showing that Π belongs to a 5-dimensional irreducible representation of $Sp(4)$. The transformation of $\text{tr}[\Pi \otimes \Pi]$ therefore reads:

$$\text{tr}[\Pi \otimes \Pi] \longrightarrow \text{tr}[\Pi \otimes \Pi] + \text{tr}[M\Pi \otimes \Pi + \Pi \otimes M\Pi]$$
$$= \text{tr}[\Pi \otimes \Pi] + \Pi^T M\Pi = \text{tr}[\Pi \otimes \Pi], \tag{B4}$$

where we have used that M is antisymmetric in the last equality.

[1] Y. Hochberg, E. Kuflik, T. Volansky, and J. G. Wacker, Phys. Rev. Lett. **113**, 171301 (2014), 1402.5143.
[2] Y.-D. Tsai, R. McGehee, and H. Murayama (2020), 2008.08608.
[3] D. B. Kaplan and H. Georgi, Phys. Lett. B **136**, 183 (1984).
[4] D. B. Kaplan, H. Georgi, and S. Dimopoulos, Phys. Lett. B **136**, 187 (1984).
[5] M. J. Dugan, H. Georgi, and D. B. Kaplan, Nucl. Phys. B **254**, 299 (1985).
[6] W. A. Bardeen, C. N. Leung, and S. T. Love, Phys. Rev. Lett. **56**, 1230 (1986).
[7] C. N. Leung, S. T. Love, and W. A. Bardeen, Nucl. Phys.

B **273**, 649 (1986).
[8] K. Yamawaki, M. Bando, and K.-i. Matumoto, Phys. Rev. Lett. **56**, 1335 (1986).
[9] S. Weinberg, Phys. Rev. D **13**, 974 (1976), [Addendum: Phys.Rev.D 19, 1277–1280 (1979)].
[10] L. Susskind, Phys. Rev. D **20**, 2619 (1979).
[11] D. Buarque Franzosi, G. Cacciapaglia, and A. Deandrea, Eur. Phys. J. C **80**, 28 (2020), 1809.09146.
[12] Y. Aoki, T. Aoyama, M. Kurachi, T. Maskawa, K.-i. Nagai, H. Ohki, E. Rinaldi, A. Shibata, K. Yamawaki, and T. Yamazaki (LatKMI), Phys. Rev. Lett. **111**, 162001 (2013), 1305.6006.
[13] Y. Aoki et al. (LatKMI), Phys. Rev. D **89**, 111502 (2014),

1403.5000.

[14] Z. Fodor, K. Holland, J. Kuti, S. Mondal, D. Nogradi, and C. H. Wong, PoS **LATTICE2014**, 244 (2015), 1502.00028.

[15] R. C. Brower, A. Hasenfratz, C. Rebbi, E. Weinberg, and O. Witzel, Phys. Rev. D **93**, 075028 (2016), 1512.02576.

[16] R. Arthur, V. Drach, A. Hietanen, C. Pica, and F. Sannino (2016), 1607.06654.

[17] A. Hasenfratz, C. Rebbi, and O. Witzel, Phys. Lett. B **773**, 86 (2017), 1609.01401.

[18] T. Appelquist et al., Phys. Rev. D **93**, 114514 (2016), 1601.04027.

[19] A. Athenodorou, E. Bennett, G. Bergner, D. Elander, C. J. D. Lin, B. Lucini, and M. Piai, PoS **LATTICE2016**, 232 (2017), 1702.06452.

[20] T. Appelquist et al. (Lattice Strong Dynamics), Phys. Rev. D **99**, 014509 (2019), 1807.08411.

[21] J.-W. Lee, E. Bennett, D. K. Hong, C. J. D. Lin, B. Lucini, M. Piai, and D. Vadacchino, PoS **LATTICE2018**, 192 (2018), 1811.00276.

[22] E. Bennett, D. K. Hong, J.-W. Lee, C. J. D. Lin, B. Lucini, M. Piai, and D. Vadacchino, JHEP **12**, 053 (2019), 1909.12662.

[23] T. Appelquist et al. (LSD) (2021), 2106.13534.

[24] V. Drach, T. Janowski, C. Pica, and S. Prelovsek, JHEP **04**, 117 (2021), 2012.09761.

[25] G. Cacciapaglia and F. Sannino, JHEP **04**, 111 (2014), 1402.0233.

[26] G. Cacciapaglia, C. Pica, and F. Sannino, Phys. Rept. **877**, 1 (2020), 2002.04914.

[27] J. Bijnens and J. Lu, JHEP **03**, 028 (2011), 1102.0172.

[28] L. Del Debbio, A. Patella, and C. Pica, Phys. Rev. D **81**, 094503 (2010), 0805.2058.

[29] K. G. Wilson, Phys. Rev. D **10**, 2445 (1974).

[30] B. Sheikholeslami and R. Wohlert, Nucl. Phys. B **259**, 572 (1985).

[31] M. Lüscher and P. Weisz, Commun. Math. Phys. **97**, 59 (1985), [Erratum: Commun.Math.Phys. 98, 433 (1985)].

[32] R. Arthur, V. Drach, M. Hansen, A. Hietanen, C. Pica, and F. Sannino, Phys. Rev. D **94**, 094507 (2016), 1602.06559.

[33] G. Martinelli, C. Pittori, C. T. Sachrajda, M. Testa, and A. Vladikas, Nucl. Phys. B **445**, 81 (1995), hep-lat/9411010.

[34] T. A. Ryttov and F. Sannino, Phys. Rev. D **78**, 115010 (2008), 0809.0713.

[35] M. Lüscher and U. Wolff, Nucl. Phys. B **339**, 222 (1990).

[36] M. Lüscher, Commun. Math. Phys. **105**, 153 (1986).

[37] M. Lüscher, Nucl. Phys. B **354**, 531 (1991).

[38] M. Lüscher, Nucl. Phys. B **364**, 237 (1991).

[39] K. Rummukainen and S. A. Gottlieb, Nucl. Phys. B **450**, 397 (1995), hep-lat/9503028.

[40] C. h. Kim, C. T. Sachrajda, and S. R. Sharpe, Nucl. Phys. B **727**, 218 (2005), hep-lat/0507006.

[41] S. He, X. Feng, and C. Liu, JHEP **07**, 011 (2005), hep-lat/0504019.

[42] V. Bernard, M. Lage, U. G. Meißner, and A. Rusetsky, JHEP **01**, 019 (2011), 1010.6018.

[43] R. A. Briceño and Z. Davoudi, Phys. Rev. D **88**, 094507 (2013), 1204.1110.

[44] R. A. Briceño, Phys. Rev. D **89**, 074507 (2014), 1401.3312.

[45] F. Romero-López, A. Rusetsky, and C. Urbach, Phys. Rev. D **98**, 014503 (2018), 1802.03458.

[46] T. Luu and M. J. Savage, Phys. Rev. D **83**, 114508 (2011), 1101.3347.

[47] M. Göckeler, R. Horsley, M. Lage, U. G. Meißner, P. E. L. Rakow, A. Rusetsky, G. Schierholz, and J. M. Zanotti, Phys. Rev. D **86**, 094513 (2012), 1206.4141.

[48] R. A. Briceño, J. J. Dudek, and R. D. Young, Rev. Mod. Phys. **90**, 025001 (2018), 1706.06223.

[49] D. Guo, A. Alexandru, R. Molina, M. Mai, and M. Döring, Phys. Rev. D **98**, 014507 (2018), 1803.02897.

[50] Z. Fu and X. Chen, Phys. Rev. D **98**, 014514 (2018), 1712.02219.

[51] M. Mai, C. Culver, A. Alexandru, M. Döring, and F. X. Lee, Phys. Rev. D **100**, 114514 (2019), 1908.01847.

[52] R. A. Briceño, J. J. Dudek, R. G. Edwards, and D. J. Wilson, Phys. Rev. D **97**, 054513 (2018), 1708.06667.

[53] L. Liu et al., Phys. Rev. D **96**, 054516 (2017), 1612.02061.

[54] T. Iritani, S. Aoki, T. Doi, T. Hatsuda, Y. Ikeda, T. Inoue, N. Ishii, H. Nemura, and K. Sasaki, Phys. Rev. D **96**, 034521 (2017), 1703.07210.

[55] M. Lüscher, Commun. Math. Phys. **104**, 177 (1986).

[56] S. König and D. Lee, Phys. Lett. B **779**, 9 (2018), 1701.00279.

[57] J. Bijnens and J. Lu, JHEP **11**, 116 (2009), 0910.5424.

[58] T. D. Blanton, F. Romero-López, and S. R. Sharpe, Phys. Rev. Lett. **124**, 032001 (2020), 1909.02973.

[59] A. Gómez Nicola, J. R. Peláez, and G. Ríos, Phys. Rev. D **77**, 056006 (2008), 0712.2763.